

News on the nuclear structure of neutron-rich nuclei at and beyond $N=28$

Alexandra Gade

National Superconducting Cyclotron Laboratory and Department of Physics and Astronomy,
Michigan State University, East Lansing, MI 48824, USA

E-mail: gade@msu.edu

Abstract. The nuclear potential and resulting shell structure are well established for the valley of stability, however, dramatic modifications to the familiar ordering of single-particle orbitals in rare isotopes with a large imbalance of proton and neutron numbers have been found: new shell gaps emerge and conventional magic numbers are no longer valid. This article outlines some of the recent in-beam γ -ray spectroscopy measurements at NSCL aimed at shedding light on the evolution of nuclear structure around neutron number $N = 28$ in neutron-rich Ar and S isotopes.

(Received April 2, 2018)

1. Introduction

Experiments on neutron-rich Si, S, and Ar isotopes continue to revolutionize our understanding of the changes in nuclear structure encountered at the extremes of isospin [1, 2, 3, 4], starting with the observation that the $N = 28$ shell closure may not persist for neutron-rich nuclei more than 20 years ago [5, 6] and continuing today with the discovery of shape [7] and configuration coexistence [8, 9, 10, 11] in ^{44}S , for example.

Recent experiments at the NSCL [12] used in-beam γ -ray spectroscopy with fast beams of rare isotopes [13] to explore, for key isotopes or isotopic chains, the single-particle structure from direct reactions or the detailed level structure as populated in fragmentation reactions, respectively. Figure 1 highlights, on the nuclear chart, the nuclei for which the results are reviewed in the present article.

One way of probing nuclear structure in a quantitative way is through the use of direct nuclear reactions that selectively probe specific degrees of freedom, e.g. the proton and neutron single-particle degrees of freedom. Intriguing possibilities arise when the single-particle and single-hole structure of a nucleus can be probed for protons and neutrons, using, for example, fast-beam one-nucleon pickup [14, 15, 16] and one-nucleon-knockout [17] reactions with γ -ray detection to deduce the partial cross sections for the population of individual final states. Other less selective reactions, as for example secondary fragmentation of fast projectiles, populate the low-lying excited states of nuclei and can provide a first glimpse at the excitation level schemes of exotic nuclei [13].

At NSCL, for the measurements described in the following, the γ -ray spectroscopy was performed with either GRETINA [18] or SeGA [19] in coincidence with the detection of the projectile-like reaction residues in the S800 spectrograph [20]. The γ rays emitted by the

projectiles in flight ($v/c \approx 0.3$) are detected with large Doppler shifts in the laboratory frame and the segmentation or position sensitivity of the γ -ray spectroscopy arrays is needed to event-by-event Doppler reconstruct the γ -ray transitions into the reference frame of the reaction residue. All reaction residues are identified and characterized using the particle's time of flight and energy loss as measured with beam line timing scintillators and the S800 focal-plane detection system.

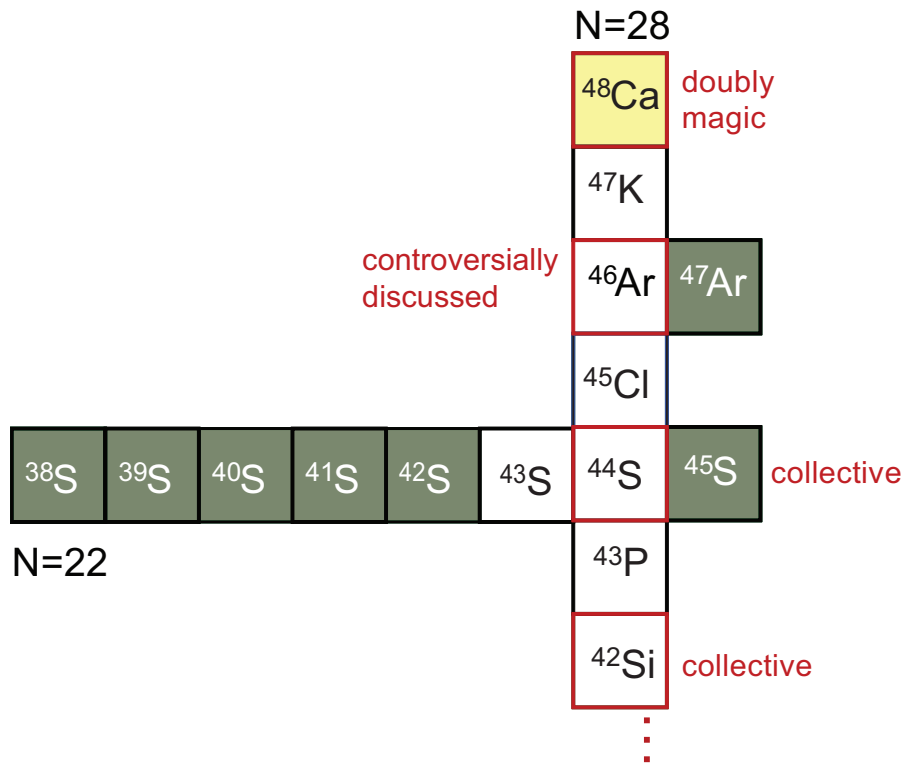


Figure 1. (Color online) Rapid shell evolution has been observed along the $N = 28$ isotone line south of doubly magic ^{48}Ca as ^{42}Si is approached. Ar and S isotopes recently studied at NSCL are shaded and are the topic of this article.

The following sections briefly summarize recent experiments performed at NSCL: The study of ^{47}Ar in the one-neutron pickup reaction from ^{46}Ar and the one-proton knockout from ^{48}K [27], the first observation of excited states in ^{45}S , and the detailed study of excited-state level schemes of neutron-rich S isotopes approaching $N = 28$ from secondary fragmentation.

2. Learning from $N = 29$ – A complementary approach

The role of the Ar isotopes around $N = 28$ is of great interest. They are, with element number $Z = 18$, located between doubly-magic ^{48}Ca and the already collective S isotopes [6] ($Z = 16$) on the path toward ^{42}Si [21], which has the lowest-lying 2_1^+ state along the $N = 28$ isotonic chain.

The nucleus ^{46}Ar has challenged existing shell model calculations which overpredict the $B(E2)$ excitation strength to the first 2^+ state [5, 22, 23, 24], while describing well other observables, most recently related to masses of the Ar isotopes around $N = 28$, for example [25]. This is not without experimental controversy, where an excited-state lifetime measurement yields higher collectivity in agreement with shell model calculations [26], but disagrees with several Coulomb excitation measurements that consistently yield a lower $B(E2)$ value [5, 22, 24].

Reminded in the following is the study of ^{47}Ar using two complementary intermediate-energy nuclear reactions, $^{12}\text{C}(^{46}\text{Ar}, ^{47}\text{Ar}+\gamma)\text{X}$, and $^9\text{Be}(^{48}\text{K}, ^{47}\text{Ar}+\gamma)\text{X}$ and the first spectroscopy of ^{45}S accomplished with a one-proton removal reaction from ^{46}Cl projectiles [27].

2.1. Single-neutron particle and single-proton hole strength

We have presented a comprehensive spectroscopy of ^{47}Ar performed using two complementary direct reactions, one-neutron pickup onto ^{46}Ar projectiles and one-proton removal from the 1^- ground state of ^{48}K . Both of the state-of-the-art SDPF-U and SDPF-MU shell-model effective interactions provided a good description of the data, with (a) SDPF-U in better agreement with the ^{47}Ar excitation energies and the location of the neutron spectroscopic strength, and (b) SDPF-MU describing better the ^{47}Ar yield from proton removal from the $2s_{1/2}$ orbital in the ^{48}K ground state [27]. Figure 2 summarizes the results.

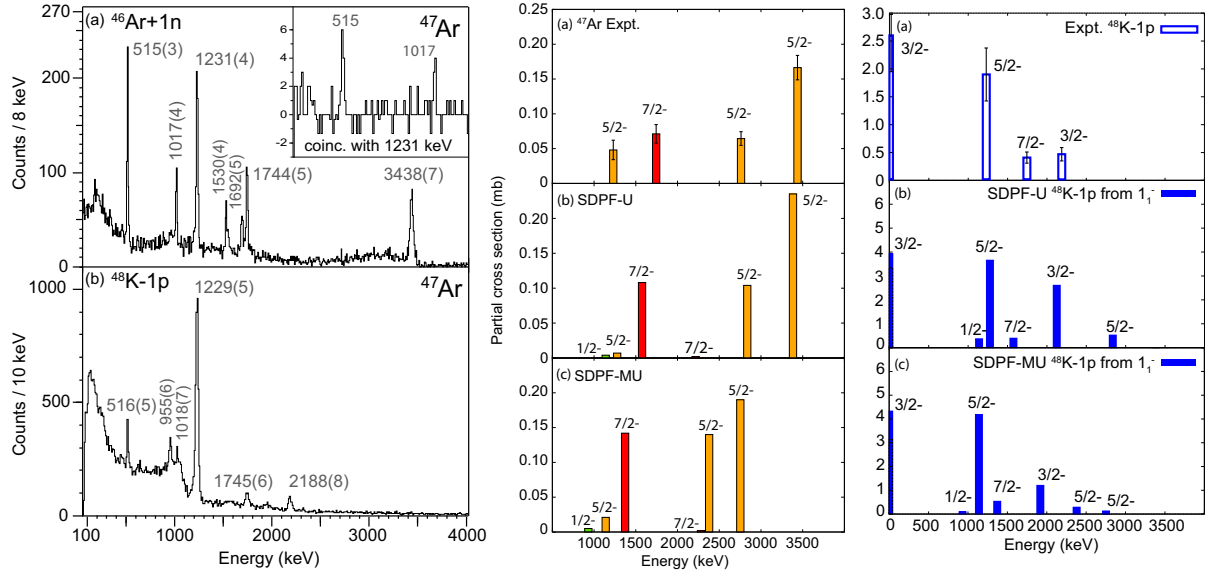


Figure 2. (Color online) Left: ^{47}Ar γ -ray spectra as observed following the (a) one-neutron pickup onto ^{46}Ar projectiles (using GREINA) and (b) one-proton removal from ^{48}K projectiles (using SeGA). Middle and right: comparison of measured and calculated cross sections using nuclear structure input from two different effective shell model interactions. Details are given in Ref. [27]. Figure adapted from [27].

2.2. Reaching the furthest in the chain of S isotopes

From the $^9\text{Be}(^{46}\text{Cl}, ^{45}\text{S}+\gamma)\text{X}$ one-proton removal reaction, the first observation of γ -ray transitions in ^{45}S was accomplished. This makes ^{45}S the most neutron-rich odd- A sulfur isotope with spectroscopic information available, while ^{46}S is still the heaviest S isotope successfully accessed with γ -ray spectroscopy [28] to date. From comparisons with shell model calculations, and arguments based on intensities and energy sums, a first tentative level scheme for ^{45}S was proposed. The ^{45}S γ -ray spectrum is broadly consistent with expectations when assuming a 1^- ^{46}Cl ground-state spin and the corresponding proton spectroscopic factors from the SDPF-U interaction. Opportunities to advance our understanding of the $N = 29$ nucleus ^{45}S will emerge once the ground-state spin of ^{46}Cl is known, after which a more quantitative analysis, as done for ^{47}Ar , can be performed for the one-proton removal data [27]. Figure 3 shows the

γ -ray spectrum as Doppler-reconstructed with SeGA and the particle identification spectrum that used information from the S800 spectrograph.

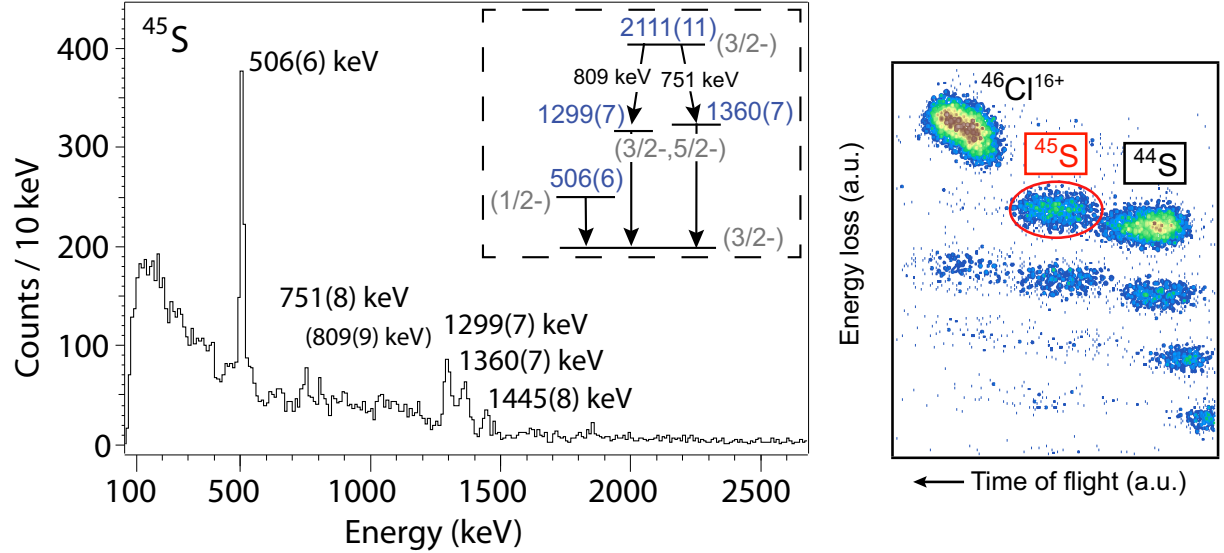


Figure 3. (Color online) Left: Gamma-ray spectrum observed with SeGA in coincidence with ^{45}S and tentative level scheme. No γ -ray transitions were known before. Right: Particle identification spectrum of ^{45}S . Details are given in Ref. [27]. Figure adapted from [27].

3. Approaching $N = 28$ in the chain of S isotopes

We have performed in-beam γ -ray spectroscopy on neutron-rich sulfur isotopes populated by fragmentation of intermediate-energy ^{48}Ca and ^{46}Ar projectile beams. New transitions were identified in $^{39-42}\text{S}$ and new level schemes for $^{40-42}\text{S}$ were proposed from $\gamma\gamma$ coincidence information, energy sums and comparison to shell model. Shell-model calculations with the SDPF-MU Hamiltonian provided remarkable agreement and consistency with the proposed level schemes. For the odd-mass ^{41}S , a level scheme is presented that appears complete below 2.2 MeV and consistent with the predictions by SDPF-MU shell-model Hamiltonian (see Figure 4); this is a remarkable benchmark given the rapid shell and shape evolution prevalent in this textbook isotopic chain as the diminished $N = 28$ shell gap is approached.

As detailed in Ref. [29], for the even-mass S isotopes, the evolution of the yrast sequence was discussed in terms of $E(6^+)/E(2^+)$ and $E(4^+)/E(2^+)$ energy ratios. For ^{42}S , a candidate for the 2_2^+ state could be proposed that displays a unique decay branching as compared to the lighter $^{38,40}\text{S}$. This was shown to be rooted in its neutron single-particle structure and confirmed by the SDPF-MU shell-model calculations.

As to the population of excited states in fragmentation reactions, a consistent picture emerged. Transitions from yrast states were most prominent, evident even at low statistics. For the higher statistics cases, e.g. $^{40,41,42}\text{S}$, the presence of many weaker transitions became apparent that most certainly feed the low-lying level schemes. While this may always have been the assumption behind the population of excited states in fragmentation reactions, evidence was presented for the many feeding transitions that have remained unobserved in previous work discussing fragmentation reactions specifically for S isotopes [30]. In the case of $^{41}\text{S}(^{42}\text{S})$, all calculated negative(positive) parity states below 2.2 MeV(3.5 MeV) were matched to states of the proposed level schemes, including off-yrast states. A number of weaker transitions remained unplaced.

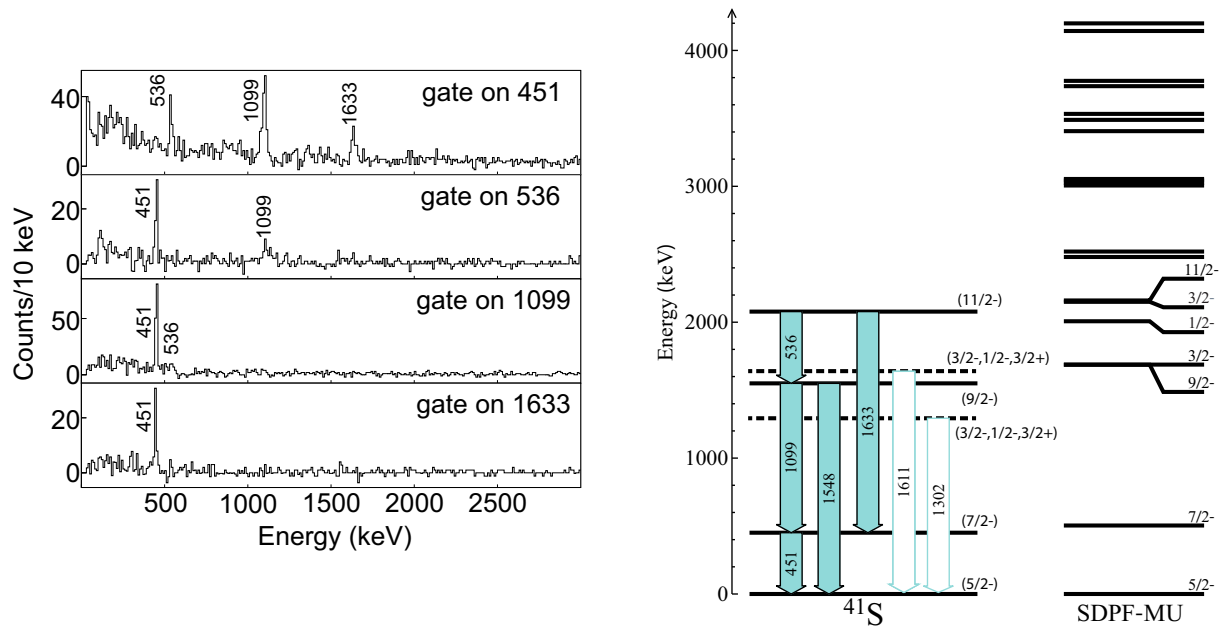


Figure 4. (Color online) Gamma-ray coincidence spectra for ^{41}S (left) and resulting level scheme compared to shell model calculations (right). Unfilled arrows indicate tentative placement of transitions. Details are given in Ref. [29]. Figure adapted from [29].

4. Summary

Neutron-rich Ar and S nuclei continue to provide important benchmarks for nuclear theory in the quest to unravel the driving forces of shell and shape evolution. The results from recent in-beam γ -ray spectroscopy studies on ^{47}Ar , ^{45}S , and $^{38-42}\text{S}$ were reviewed. In general, very good agreement between measured results and large-scale shell model calculations was demonstrated.

Acknowledgments

This work was supported by the National Science Foundation under Grants No. PHY-1565546. Over the many years, more than a decade by now, valuable collaboration and countless inspiring discussions with Takaharu Otsuka are acknowledged that have shaped the in-beam γ -ray spectroscopy program at NSCL.

References

- [1] Utsuno Y et al. 2012 *Phys. Rev. C* **86** 051301
- [2] Nowacki F and Poves A 2009 *Phys. Rev. C* **79** 014310
- [3] Sorlin O and Porquet M-G 2013 *Phys. Scr.* **T152** 014003
- [4] Gade A and Liddick SN 2016 *J. Phys. G: Nucl. Part. Phys.* **43** 024001
- [5] Scheit H et al. 1996 *Phys. Rev. Lett.* **77** 3967
- [6] Glasmacher T et al. 1997 *Phys. Lett. B* **395** 163
- [7] Force C et al. 2010 *Phys. Rev. Lett.* **105** 102501
- [8] Santiago-Gonzalez D et al. 2011 *Phys. Rev. C* **83** 061305(R)
- [9] Utsuno Y et al. 2015 *Phys. Rev. Lett.* **114** 032501
- [10] Egido JL et al. 2016 *Phys. Rev. Lett.* **116** 052502
- [11] Parker JJ et al. 2017 *Phys. Rev. Lett.* **118** 052501
- [12] Gade A and Sherrill BM 2016 *Phys. Scr.* **91** 053003
- [13] Gade A and Glasmacher T 2008 *Prog. Part. Nucl. Phys.* **60** 161
- [14] McDaniel S et al. 2012 *Phys. Rev. C* **85** 014610
- [15] Gade A et al. 2011 *Phys. Rev. C* **83** 054324

- [16] Gade A et al. 2007 *Phys. Rev. C* **76** 061302(R)
- [17] Hansen PG and Tostevin JA 2003 *Annu. Rev. Nucl. Part. Sci.* **53** 221
- [18] Weisshaar D et al. 2017 *Nuclear Instrum. Methods Phys. Res. A* **847** 187
- [19] Mueller WF et al. 2001 *Nuclear Instrum. Methods Phys. Res. A* **466** 492
- [20] Bazin D et al. 2003 *Nuclear Instrum. Methods in Phys. Res. B* **204** 629
- [21] Bastin B et al. 2007 *Phys. Rev. Lett.* **99** 022503
- [22] Gade A et al. 2003 *Phys. Rev. C* **68** 014302
- [23] Winkler R et al. 2012 *Phys. Rev. Lett.* **108** 182501
- [24] Calinescu S et al. 2016 *Phys. Rev. C* **93** 044333
- [25] Meisel Z et al. 2015 *Phys. Rev. Lett.* **114** 022501
- [26] Mengoni D et al. 2010 *Phys. Rev. C* **82** 024308
- [27] Gade A et al. 2016 *Phys. Rev. C* **93** 054315
- [28] Gade A et al. 2009 *Phys. Rev. Lett.* **102** 182502
- [29] Lunderberg E et al. (2016) *Phys. Rev. C* **94** 064327
- [30] Sohler D et al. 2002 *Phys. Rev. C* **66** 054302